Chapter 6

Correlation Between Band Structure and Magneto-Transport Properties in n-type HgTe/CdTe Two-Dimensional Nanostructure Superlattice. Application to Far-Infrared Detection

Abdelhakim Nafidi

Additional information is available at the end of the chapter

http://dx.doi.org/10.5772/52101

1. Introduction

The work of Essaki & Tsu [1] caused a big interest to the study of superlattices made from alternating layers of two semiconductors. The development of molecular beam epitaxy (MBE) was successfully applied to fabricate different quantum wells and superlattices. Among them III-V superlattices [$Ga_{1-x}Al_xAs$-GaAs [1-2] - type I], III-V superlattices [InAs/GaSb [3] - type II] and later II-VI superlattice [HgTe/CdTe [4] - type III]. The latter is a stable alternative for application in infrared optoelectronic devices than the $Hg_{1-x}Cd_xTe$ alloys. Especially in the region of second atmospheric window (around 10 μm) which is of great interest for communication.

HgTe and CdTe crystallize in zinc –blend lattice respectively. The lattice-matching within 0.3 % yield to a small interdiffusion between HgTe and CdTe layers at low temperature near 200 °C by MBE. HgTe is a zero gap semiconductor (due to the inversion of relative positions of Γ_6 and Γ_8 edges [5]) when it is sandwiched between the wide gap semiconductor CdTe (1.6 eV at 4.2 K) layers yield to a small gap HgTe/CdTe superlattice which is the key of an infrared detector.

A number of papers have been published devoted to the band structure of this system [6] as well as its magnetooptical and transport properties [7]. The aim of this work is to show the correlation between calculated bands structures and magneto- transport properties in n type HgTe/CdTe nanostructures superlattices. The interpretation of the experimental data is consistent with the small positive offset Λ=40 meV between the HgTe and CdTe valence bands.

Theoretical calculations of the electronic properties of n-type HgTe/CdTe superlattices (SLs) have provided an agreement with the experimental data on the magneto-transport behaviour. We have measured the conductivity, Hall mobility, Seebeck and Shubnikov-de Haas effects and angular dependence of the magneto-resistance [8]. Our sample, grown by MBE, had a period $d=d_1+d_2$ (124 layers) of d_1=8.6 nm (HgTe) /d_2=3.2 nm (CdTe). Calculations of the spectres of energy $E(d_2)$, $E(k_z)$ and $E(k_p)$, respectively, in the direction of growth and in plane of the superlattice; were performed in the envelope function formalism. The energy $E(d_2, \Gamma, 4.2\ K)$, shown that when d_2 increase the gap E_g decrease to zero at the transition semiconductor to semimetal conductivity behaviour and become negative accusing a semimetallic conduction. At 4.2 K, the sample exhibits n type conductivity, confirmed by Hall and Seebeck effects, with a Hall mobility of 2.5 10^5 cm^2/Vs. This allowed us to observe the Shubnikov-de Haas effect with n = 3.20 10^{12} cm^{-2}. Using the calculated effective mass ($m^*_{E1}(E_F) = 0.05\ m_0$) of the degenerated electrons gas, the Fermi energy (2D) was E_F=88 meV in agreement with 91 meV of thermoelectric power α. In intrinsic regime, $\alpha\ T^{-3/2}$ and $R_H T^{3/2}$ indicates a gap $E_g = E_1 - HH_1$= 101 meV in agreement with calculated $E_g(\Gamma, 300\ K)$ =105 meV The formalism used here predicts that the system is semiconductor for $d_1/d_2 = 2.69$ and $d_2 < 100$ nm. Here, d_2=3.2 nm and E_g (Γ,4.2 K) = 48 meV so this sample is a two-dimensional modulated nano-semiconductor and far-infrared detector (12 μm<λ_c<28 μm).

In conclusion, we will show that the HgTe/CdTe nano-superlattice is a stable alternative for application in infrared optoelectronic devices than the alloys $Hg_{1-x}Cd_xTe$.

2. Experimental techniques

The HgTe/CdTe superlattice was grown by molecular beam epitaxy (MBE) on a [111] CdTe substrate at 180 °C. The sample (124 layers) had a period $d=d_1+d_2$ where d_1(HgTe)=8.6 nm and d_2(CdTe)= 3.2 nm. It was cut from the epitaxial wafer with a typical sizes of 5x1x1mm^3. The ohmic contacts were obtained by chemical deposition of gold from a solution of tetrachloroauric acid in methanol after a proper masking to form the Hall crossbar. Carriers transport properties were studied in the temperature range 1.5-300K in magnetic field up to 17 Tesla. Conductivity, Hall Effect, Seebeck effect and angular dependence of the transverse magnetoresistance were measured. The measurements at weak magnetic fields (up to 1.2 T) were performed into standard cryostat equipment. The measurements of the magnetoresistance were done under a higher magnetic field (up to 8 T), the samples were immersed in a liquid helium bath, in the centre of a superconducting coil. Rotating samples with respect to the magnetic field direction allowed one to study the angular dependence of the magnetoresistance.

3. Theory of structural bands

Calculations of the spectra of energy E (k_z) and E(k_p), respectively, in the direction of growth and in plane of the superlattice; were performed in the envelope function formalism [6-7])

http://dx.doi.org/10.5772/52101

with a valence band offset Λ between heavy holes bands edges of HgTe and CdTe of 40 meV determined by the magneto-optical absorption experiments [9].

The general dispersion relation of the light particle (electron and light hole) subbands of the superlattice is given by the expression [6]:

$$\cos k_z(d_1+d_2) = \cos(k_1 d_1)\cos(k_2 d_2) - \frac{1}{2}\left[\left(\xi+\frac{1}{\xi}\right)+\frac{k_p^2}{4k_1k_2}\left(r+\frac{1}{r}-2\right)\right]\sin(k_1 d_1)\sin(k_2 d_2) \quad (1)$$

where the subscripts 1 and 2 refer to HgTe and CdTe respectively. k_z is the superlattice wave vector in the direction parallel to the growth axis z. The two-dimensional wave vector $k_p(k_x, k_y)$ describes the motion of particles perpendicular to k_z. Here,

$$\xi = \frac{k_1}{k_2} \quad \text{and} \quad r=\frac{E-\varepsilon_2}{E+|\varepsilon_1|-\Lambda} \quad (2)$$

E is the energy of the light particle in the superlattice measured from the top of the Γ_8 valence band of bulk CdTe, while εi (i =1 or 2) is the interaction band gaps $E(\Gamma_6) - E(\Gamma_8)$ in the bulk HgTe and CdTe respectively. At given energy, the two–band Kane model [10] gives the wave vector $(k_i^2+k_p^2)$ in each host material:

$$\left.\begin{aligned} \frac{2}{3}P^2\hbar^2(k_1^2+k_p^2) &= (E-\Lambda)(E-\Lambda+|\varepsilon_1|) \quad \text{for HgTe} \\ \frac{2}{3}P^2\hbar^2(k_2^2+k_p^2) &= E(E-\varepsilon_2) \quad \text{for CdTe} \end{aligned}\right\} \quad (3)$$

P is the Kane matrix element given by the relation:

$$\frac{2P^2}{3|\varepsilon_1|} = \frac{1}{2m^*} \quad (4)$$

where $m^* = 0.03\ m_0$ is the electron cyclotron mass in HgTe [5]. For a given energy E, a superlattice state exists if the right-hand side of Eq. (1) lies in the range [-1,1]. That implies $-\pi/d \le k_z \le -\pi/d$ in the first Brillion zone.

The heavy hole subbands of the superlattice are given by the same Eq. (1) with :

$$\xi = \frac{k_1}{k_2}r, \textit{ and } \quad r=1 \quad \text{with} \begin{cases} -\dfrac{\hbar^2(k_1^2+k_p^2)}{2\,m^*_{HH}} = E-\Lambda & \text{for HgTe} \\ -\dfrac{\hbar^2(k_2^2+k_p^2)}{2\,m^*_{HH}} = E & \text{for CdTe} \end{cases} \quad (5)$$

$m^*_{HH} = 0.3\ m_0$ [5] is the effective heavy hole mass in the host materials.

The band structure computation consists of solving Eq. (1) which represents the dispersion relations (i.e. finding the values of energy E which are roots of the Eq. (1) for a given value

of the carrier wave vector). Here, we are interested in studying the states of energy of light particles and heavy holes in HgTe/CdTe superlattice as function of k_z when k_p=0 and as function of k_p when k_z=0 and when k_z=π/d. The solving procedure used for studying E as function k_z in the case where k_p=0 consists of going, with a steep E, through the studied range of energy E and then finding, for each value of E,

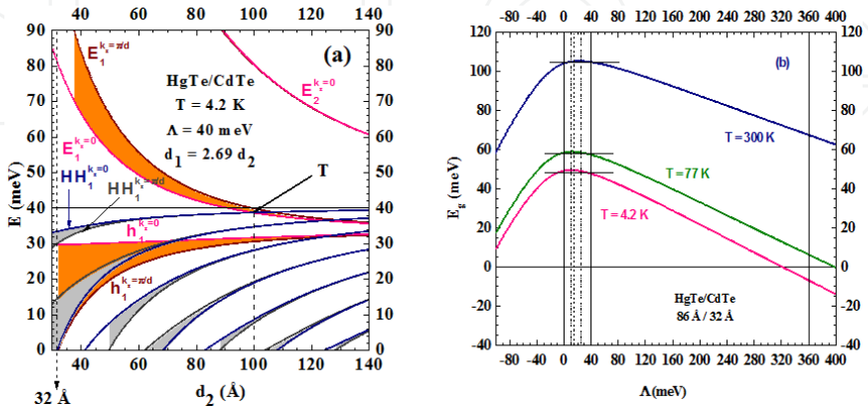

Figure 1. a) Energy position and width of the conduction (Ei), heavy-hole (HHi), and the first light-hole (h_1) subbands calculated at 4,2 K in the first Brillion zone as a function of layer thickness for HgTe/CdTe superlattice with d_1=2.69 d_2, where d_1 and d_2 are the thicknesses of the HgTe and CdTe layers, respectively. T is the point of the transition semiconductor- semimetal. (b) the band gap E_g (Γ) at Γ, as function of temperature and valence band offset Λ between heavy holes bands edges of HgTe and CdTe for the investigated HgTe/CdTe superlattice.

the value of k_z which satisfies the dispersion relations. The same procedure is used for studying E as function k_p in the case where k_z=0 and k_z=π/d. It is noteworthy that, for a given value of E, Eq. (1) may have more than one root in k_p. It appears, from Eq. (3)-(5), that the carrier wave vectors k_1, k_2, and k_p are either real or imaginary (i.e. complex) and then using complex numbers in the calculation seems to be more adequate.

4. Theoretical results and discussions

The energy E as a function of d_2, at 4.2 K, in the first Brillion zone and for d_1 = 2.69 d_2, is shown in "Figure 1 (a)". The case of our sample (d_2 = 32 Å) is indicated by the vertical solid line. Here the cross-over of E_1 and HH_1 subbands occurs. d_2 controls the superlattice band gap $E_g = E_1$-HH_1. For weak d_2 the sample is semiconductor with a strong coupling between the HgTe wells. At the point T(d_2 = 100 Å, E= 38 meV) the gap goes to zero with the transition semiconductor- semimetal. When d_2 increases, E_1 and h_1 states drops in the energy gap [0, Λ] and become interface state with energy

$$E_I = \frac{\Lambda \varepsilon_2}{|\varepsilon_1| + \varepsilon_2} = 34\, meV \tag{6}$$

http://dx.doi.org/10.5772/52101

for infinite d_2 obtained from Eq. (1). Then the superlattice has the tendency to become a layer group of isolated HgTe wells and thus assumes a semimetallic character. The ratio d_1/d_2 governs the width of superlattice subbands (i.e. the electron effective mass). A big d_1/d_2, as in the case of 4.09 in Fig. 2, moves away the material from the two-dimensional behaviour.

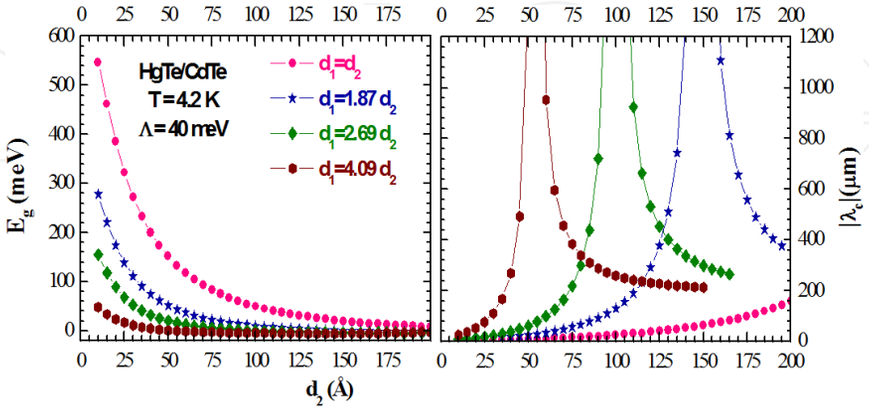

Figure 2. E_g (Γ) and $|\lambda_c|$ as function of d_2 for various d_1/d_2 at 4.2 K.

In "Figure 1 (b)" we can see that the band gap $E_g(\Gamma)$ increases, presents a maximum at 10, 15 and 25 meV respectively for 4.2, 77 and 300K, near Λ=40 meV and decreases when the valence band offset Λ between heavy hole band edges of HgTe and CdTe increase. For each Λ, $E_g(\Gamma)$ increases with T. Our chosen value of 40 meV is indicated by a vertical solid line. This offset agrees well with our experimental results and 0 meV used by [4] for all temperatures, indicated by a horizontal solid line in "Figure 1 (b)", contrary to 360 meV given by [11]. The later offset give E_g = -8 meV in "Figure 1 (b)" whereas, in intrinsic regime, $R_H T^{3/2}$ indicates a measured gap $E_g \approx 98$ meV in agreement with our calculated $E_g(\Gamma,300\ K) = 105$ meV.

"Figure 2" shows that, for each d_2, E_g (Γ) decreases when d_1/d_2 increases. For each d_1/d_2, when d_2 increases E_g (Γ) decreases, go to zero at the transition point T and became negative for a semimetal conductivity. In the right of "Figure 2", the cut-off wavelength $|\lambda_c|$ diverge at T with d_2=54 Å, 100 Å, 150 Å,... respectively for d_1/d_2=4.09, 2.69, 1.87, … So, the transition goes to high d_2 when d_1/d_2 decreases. In the case of our sample the transition occur at d_2 =100 Å.

Using the value of ε_1 and ε_2 at different temperatures between 4.2 K and 300 K [12] and taking P temperature independent, this is supported by the fact that from eq.(4) $P \approx \varepsilon_G(T)/m^*(T) \approx$ Cte, we get the temperature dependence of the band gap Eg, in the centre Γ of the first Brillouin zone in "Figure 3". Note that E_g increases from 48 meV at 4.2 K to 105 meV at 300 K. We calculated the detection cut-off wave length by the relation

$$\lambda_c(\mu m) = \frac{1240}{E_g(meV)} \tag{7}$$

In the investigated temperature range 12 μm < λ_c < 28 μm situates our sample as a far infrared detector.

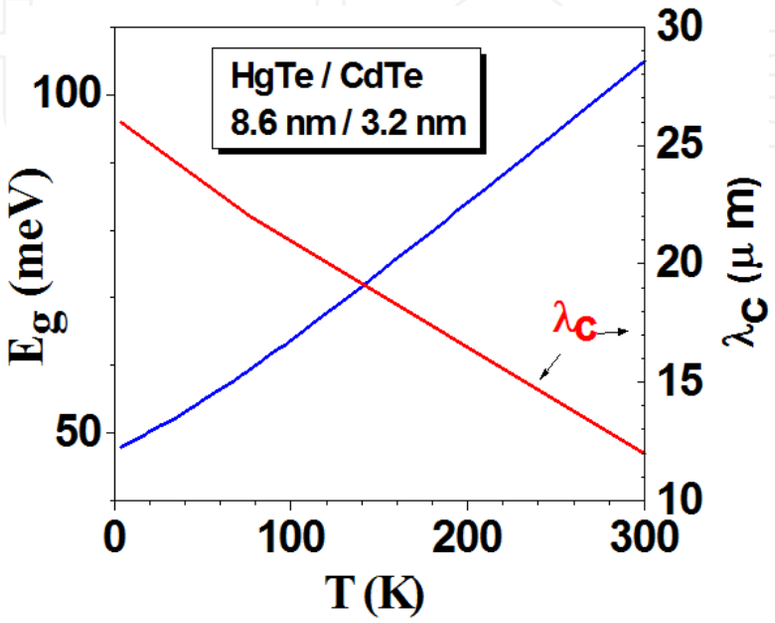

Figure 3. Temperature dependence of the band gap E_g and the cut-off wavelength λ_c, at the center Γ of the first Brillouin zone.

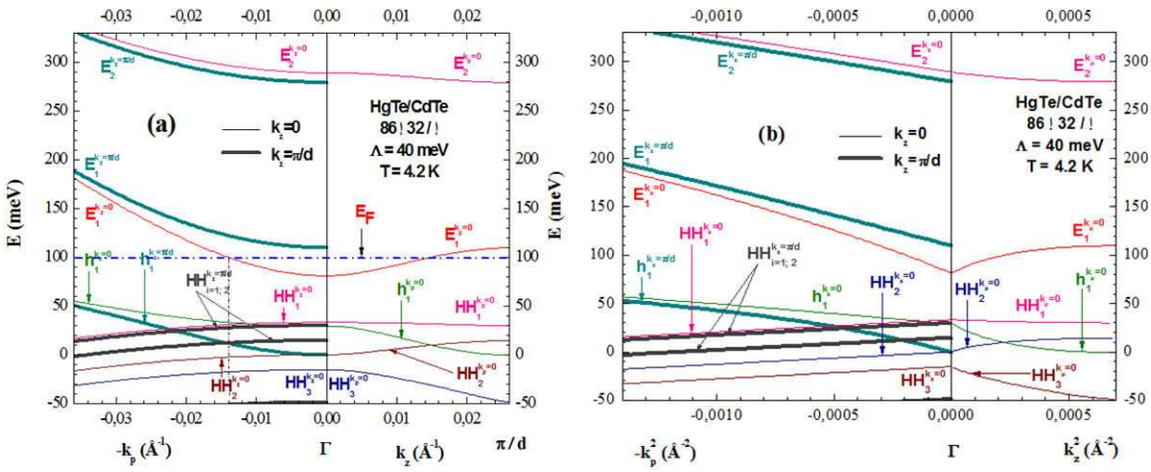

Figure 4. a) Calculated bands along the wave vector k_z in the right and in plane $k_p(k_x,k_y)$ for k_z=0 and π/d in the left,. E_F is the energy of Fermi level. (b) Calculated bands along the k_z^2 in the right and k_p^2 for k_z=0 and π/d in the left; of the HgTe/CdTe superlattice at 4.2 K.

http://dx.doi.org/10.5772/52101

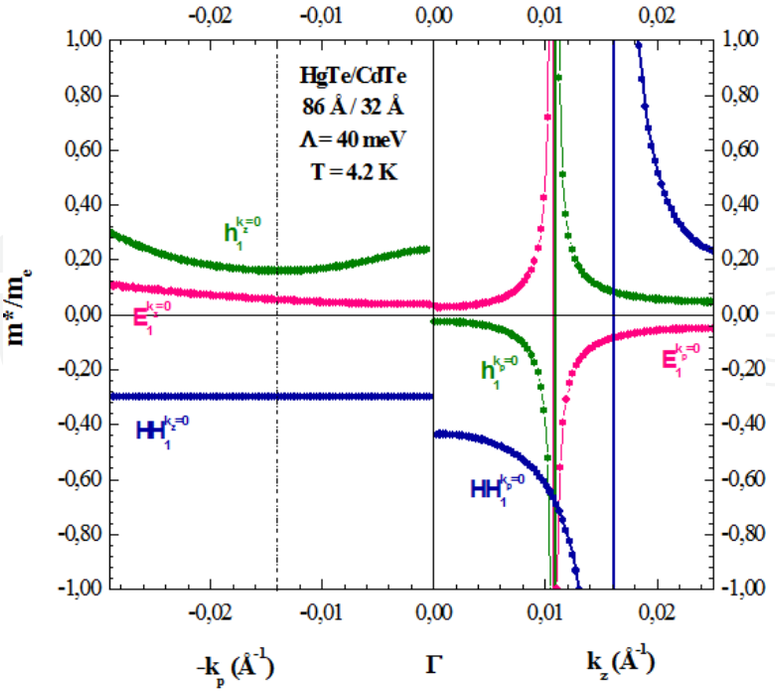

Figure 5. Calculated relative effective mass bands along the wave vector kz and in plane kp of the HgTe/CdTe superlattice at 4.2 K

In "Figure 4 (a)" we can see the spectres of energy $E(k_z)$ and $E(k_p)$, respectively, in the direction of growth and in plane of the superlattice at 4.2 K. Along k_z the subbands E_1 and h_1 are large and non-parabolic as shown in "Figure 4. (b)". Along k_p, E_1 and h_1 increase with k_p whereas the parabolic HH_n decreases in "Figure 4. (b)". This yield to an anti-crossing of HH_1 and h_1 at k_p= 0.0139 Å^{-1} near the middle of the first Brillouin zone (π/2d).

For an anisotropic medium, such as the HgTe/CdTe superlattices, the effective mass is a tensor and its elements along μ and ν directions are given by the following expression [12].

$$\left(\frac{1}{m^*}\right)_{\mu\nu} = \frac{1}{\hbar^2}\frac{\partial^2 E_{k_{\mu\nu}}}{\partial k_\mu \partial k_\nu} \tag{8}$$

By carrying out second derivative of the energy E_1, h_1 and HH_1 along k_z and k_p in "Figure 4 (a)", we calculated the effective mass bands in "Figure 5". Along k_p, the effective mass of heavy holes m^*_{HH1}= - 0.30 m_0 and the effective mass of electrons m^*_{E1} increases from 0.04 m_0 to 0.11 m_0. In "Figure 4 (a)", the Fermi level across the conduction band E_1 at k_p=0.014 Å^{-1} corresponding to

$$\left(m^*_{E_1}\right)_{E_F} = 0.05\, m_0 \tag{9}$$

from "Figure 5". Whereas, the effective mass of the light holes h_1 deceases from 0.24 m_0, to a minimum of

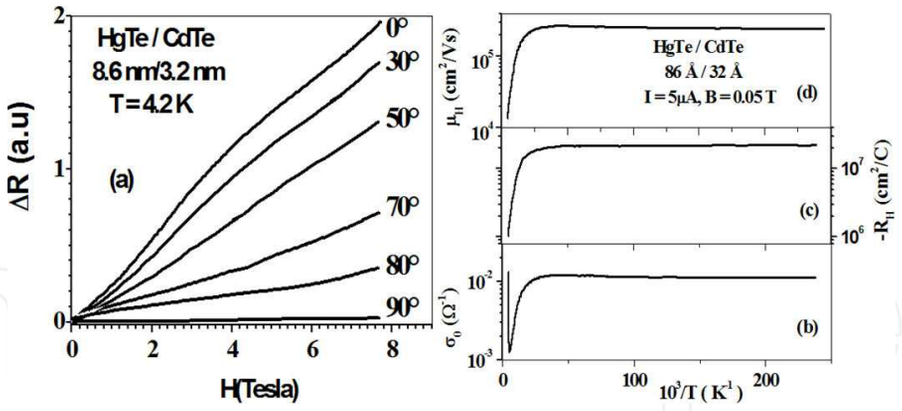

Figure 6. Variation of magnetoresistance of the sample with various angles between the magnetic field and the normal to the HgTe/CdTe superlattice surface (a). Temperature dependence of the conductivity (b), weak-field Hall coefficient (c) and Hall mobility (d) in the investigated HgTe/CdTe superlattice

$$\left(m_{h_1}^{*}\right)_{\min} = 0.16\, m_0 \tag{10}$$

at k_p=0.14 Å^{-1}, and increase to 0.30 m_0 assuming an electronic conduction.

5. Experimental results and discussions

In "Figure 6.(a)" we can see that the angular dependence of the magnetoresistance vanishes, when the field is parallel to the plane of the SL (at 90°), indicating a two dimensional (2D) behaviour supported by the observation of SDH oscillations in "Figure 8 (a)".

We have also measured the conductivity, Hall mobility and Seebeck effect. At low temperatures, the sample exhibits n type conductivity (R_H < 0) with a concentration n=1/e R_H =3.24x10^{12} cm^{-2} from "Figure 6 (c)" and in "Figure 7. (a)"; and a Hall mobility μ_n = 2.5x10^5 cm^2/Vs in "Figure 6 (d)". The plot log(μ_n)-log(T) in the "Figure 7.(b)" of the Hall mobility shows a scattering of electrons by phonons in the intrinsic regime with $\mu_H T^{1.58}$ and week activation energy at low temperature with μ_H $T^{0.05}$.

This relatively electrons high mobility allowed us to observe the Shubnikov-de Haas effect until 8 Tesla in "Figure 8 (a)". Its well knows that the oscillations of the magnetoresistance are periodic with respect to 1/B [14]. The period (1/B) is related to the concentration n of the electrons by the relation:

$$n = \frac{e}{\pi \hbar \Delta\left(\frac{1}{B}\right)} \tag{11}$$

In the insert of "Figure 8(a)" we have plotted the inverse of the minima's 1/B_m as a function of the entire n' following the formula:

http://dx.doi.org/10.5772/52101

$$\frac{1}{B_m} = \Delta\left(\frac{1}{B}\right)\left(n' + \frac{1}{2}\right) \tag{12}$$

The linear line slope gives (1/B) and n = 3.20x10^{12} cm^{-2} in good agreement with that measured by weak field Hall effect (H=0.5 KOe, I= 5μA) from "Figure 6(c)".

At low temperature, the superlattice electrons dominate the conduction in plane. The E_1 band is not parabolic with respect to k_p^2 in "Figure 4 (b)". That permits us to estimate the Fermi energy (2D) at 4.2K

$$E_F = n\pi h^2 \Big/ \left(m^*_{E_1}\right)_{E_F} = 88\,\text{meV} \tag{13}$$

The thermoelectric power (α<0) measurements shown in "Figure 8(b)" indicate n-type conductivity, confirmed by Hall Effect measurements (R_H<0) in "Figure 6(c)". At low temperature, α $T^{0.96}$ (in the top insert of "Figure 8(b)") is in agreement with Seebeck effect theory deduced from the relaxation time resolution of the Boltzmann equation [15].

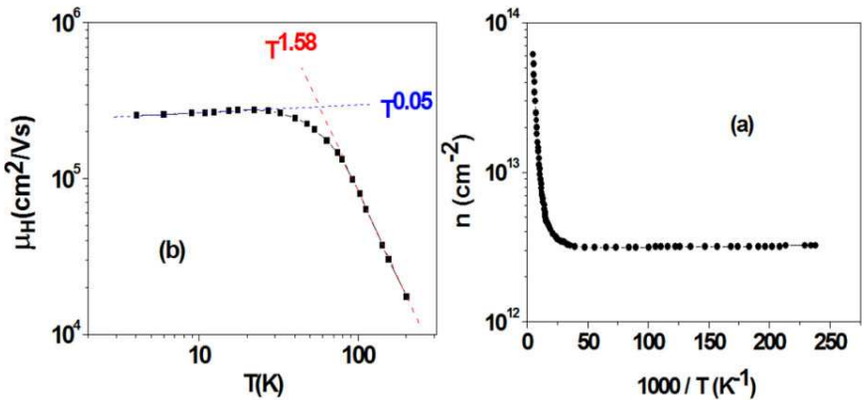

Figure 7. a) Variation with 1/T of weak-field Hall concentration and (b) Variation with T of Hall mobility in the investigated HgTe/CdTe superlattice

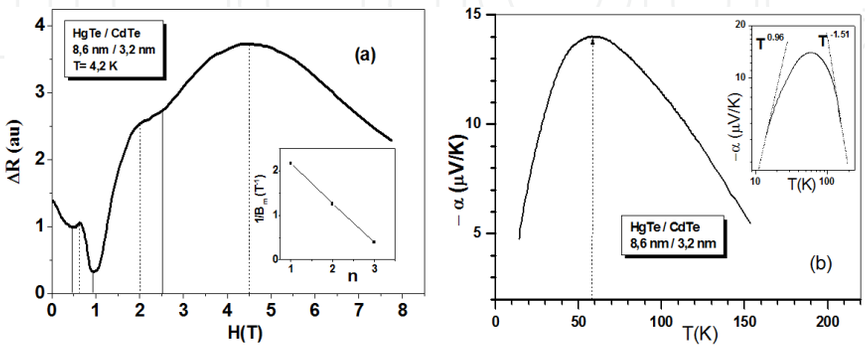

Figure 8. a) Variation of transverse magneto-resistance with magnetic field at 4.2 K, (b) Measured thermoelectric power as a function of temperature in the investigated HgTe/CdTe superlattice.

For our degenerate electrons gas the Seebeck constant is described by the formula:

$$\alpha = \frac{\left[(\pi k_B)^2 T(s+1)\right]}{3eE_F} \tag{14}$$

where the collision time τ $E^{s-(1/2)}$. This permits us to estimate the Fermi energy at E_F = 91 meV (in "Figure 4(a)"), with s= 2.03 corresponding to electrons diffusion by ionized impurities, in agreement with the calculated E_F=88 meV in formula (13). In intrinsic regime for T>150 K, the measure of the slope of the curve R_H $T^{3/2}$ indicates a gap E_g = 98 meV which agree well with calculated E_g (Γ, 300 K) = E_1-HH_1= 105 meV. Here $\alpha T^{-3/2}$ indicates electrons scattering by phonons.

This HgTe/CdTe superlattice is a stable alternative for application in far infrared optoelectronic devices than the random alloys $Hg_{0.99}Cd_{0.01}Te$ because the small composition x=0.01, with E_g (Γ, 300 K) =100 meV given by the empiric formula for $Hg_{1-x}Cd_xTe$ [16]

$$E_g(x,T) = -0{,}302+1{,}93x-0{,}810x^2+0{,}832x^3+5{,}035\times10^{-4}(1-2x)\,T \tag{15}$$

is difficult to obtain with precision while growing the ternary alloys and the transverse effective masse in superlattice is two orders higher than in the alloy. Thus the tunnel length is small in the superlattice [17].

6. Conclusions

The fundamental main ideas of this work are:

- HgTe is a zero gap semiconductor (or semimetal) when it is sandwiched between the wide gap semiconductor CdTe (1.6 eV at 4.2 K) layers yield to a narrow gap HgTe/CdTe superlattice which is the key of an infrared detector.

- Before growing our superlattice, we calculated the bands structures $E(d_2)$ and the gap for each ratio thickness d_1/d_2. After we choosed the SL in the semiconductor conductivity zone.

We reported here remarkable correlations between calculated bands structures and magneto- transport properties in HgTe/CdTe nanostructures superlattices. Our calculations of the specters of energy $E(d_2)$, $E(k_z)$ and $E(k_p)$, respectively, in the direction of growth and in plane of the superlattice; were performed in the envelope function formalism.

The formalism used here predicts that the system is semiconductor, for our HgTe to CdTe thickness ratio d_1/d_2 = 2.69, when d_2 < 100 nm. In our case, d_2=3.2 nm and E_g (Γ, 4.2 K) = 48 meV. In spite of it, the sample exhibits the features typical for the semiconductor n-type conduction mechanism. In the used temperature range, this simple is a far-infrared detector, narrow gap and two-dimensional n-type semiconductor. Note that we had observed a semimetallic conduction mechanism in the quasi 2D p type HgTe/CdTe superlattice [18].

http://dx.doi.org/10.5772/52101

In conclusion, the HgTe/CdTe superlattice is a stable alternative for application in infrared optoelectronic devices than the alloys $Hg_{1-x}Cd_xTe$.

Measurements performed by us on others' samples indicate an improvement of quality of the material manifested by higher mobility.

Author details

Abdelhakim Nafidi

Laboratory of Condensed Matter Physics and Nanomaterials for Renewable Energy University Ibn-Zohr 80000 Agadir, Morocco

References

[1] Esaki, L., & Tsu, R. (1970). Superlattice and negative differential conductivity in Semiconductors. *IBM J. Res. Development*, 1970(14), 61-65, 0018-8646.

[2] Dingle, R., Gossard, A. C., & Wiegmann, W. (1975). Direct Observation of Superlattice Formation in a Semiconductor Heterostructure. *Phys. Rev. Lett.*, 34, 1327-1330, 10.1103/PhysRevLett.34.1327.

[3] Sakaki, H., Chang, L. L., Sai-Halasz, G. A., Chang, C. A., & Esaki, L. (1978). Two-dimensional electronic structure in InAs-GaSb superlattices. *Solid State Communications*,, 26, 589-592, 10.1016/0038-1098(78)90770-6.

[4] Bastard, G. (1981). Superlattice band structure in the envelope-function approximation. *Phys. Rev. B*,, 24, 5693-5697, 10.1103/PhysRevB.24.5693.

[5] Tuchendler, J., Grynberg, M., Couder, Y., Thomé, H., & Le Toullec, R. (1973). Submillimeter Cyclotron Resonance and Related Phenomena in HgTe. *Phys. Rev. B*,, 8, 3884-3894, PhysRevB.8.3884.

[6] Bastard, G. (1982). Theoretical investigations of superlattice band structure in the envelope-function approximation. *Phys. Rev. B*,, 25, 7584-7597, 10.1103/PhysRevB. 24.5693.

[7] Nafidi, Ab., El Kaaouachi, A., Sahsah, H., & Nafidi, Ah. (2002). Band structure and magneto-transport in HgTe/CdTe superlattice. Book of the International Conference on Theoretical Physics (HT 2002). 274-275, *Birkhäuser Verlag 2000*, 3-76432-433-3.

[8] Braigue, M., Nafidi, A., Chaib, H., Devki, N., Talwar, Tirbiyine. A., Hemine, J., Idbaha, A., Boulkassim, A., El Gouti, T., Massaq, M., & Srinivasa, Vinod. M. (2011). Correlation Between Bands Structure and Magneto-Transport Properties in n-type HgTe/

CdTe Superlattice with Relatively Thin CdTe Barrier. *AIP Conference Proceedings*,, 1416,, New York: American Institute of Physics, 68-71.

[9] Guldner, Y., Bastard, G., Vieren, J. P., Voos, M., Faurie, J. P., & Million, A. (1984). Magneto-optics in a II-VI superlattice: HgTe-CdTe. *Surface Science*, 142, 593-597, 10.1016/0039-6028(84)90367-4.

[10] Kane, E. (1957). Band structure of indium antimonide. *Journal of Physics and Chemistry of Solids*,, 1(4), 249-261.

[11] Johnson, N. F., Hui, P. M., & Ehrenreich, H. (1988). Valence-Band-Offset Controversy in HgTe/CdTe Superlattices: A Possible Resolution. *Phys. Rev. Lett.*, 61(PhysRevLett. 61.1993), 1993-1995.

[12] Weiler, M. H., Willardson, R. K., & Beer, A. C. (1981). Magnetooptical Properties of $Hg_{1-x}Cd_xTe$ Alloys,. *In: semiconductors and Semimetals*, (Academic, New York)., 119-191, 978-0-12752-116-9.

[13] Kittel, C. (2001). *Introduction to solid state physics*, John Wiley and Sons, Inc, New York 333.

[14] Seeger, K. (2002). *Semiconductor physics: an introduction* [8], Springer, chap.4,, 121, 978-3-54043-813-7.

[15] Seeger, K. (2002). *Semiconductor physics: an introduction* [8], Springer, chap.6,, 159, 978-3-54043-813-7.

[16] Hansen, G. L., Schmit, J. L., & Casselman, T. N. (1982). Energy gap versus alloy composition and temperature in $Hg_{1-x}Cd_xTe$. *J. Appl. Phys*,, 53, 7099-7101, 10.1063/1.330018.

[17] Nafidi, A., et al. (2013). to be published.

[18] Braigue, M., Nafidi, A., Benlaabidya, Y., Chaib, H., Daddabi, A., Morghi, R., Idbaha, A., Massaq, M., El Gouti, T., Hemine, J., & Srinivasa, Vinod. M. (2011). Manifestation of the Transition Semiconductor-Semimetal and Intrinsic Interface State in Band Structure and Magneto-Transport Properties in Nanostructure Superlattice,. *J Supercond Nov Magn, Springer*,, 10.1007/s10948-011-1229-y.